Anal Bioanal Chem (2009) 393:1209–1216
DOI 10.1007/s00216-008-2399-8

ORIGINAL PAPER

Optical sensing in microfluidic lab-on-a-chip by femtosecond-laser-written waveguides

Rebeca Martinez Vazquez · Roberto Osellame · Marina Cretich · Marcella Chiari · Chaitanya Dongre · Hugo J. W. M. Hoekstra · Markus Pollnau · Hans van den Vlekkert · Roberta Ramponi · Giulio Cerullo

Received: 10 July 2008 / Revised: 5 September 2008 / Accepted: 9 September 2008 / Published online: 7 October 2008

Abstract We use direct femtosecond laser writing to integrate optical waveguides into a commercial fused silica capillary electrophoresis chip. High-quality waveguides crossing the microfluidic channels are fabricated and used to optically address, with high spatial selectivity, their content. Fluorescence from the optically excited volume is efficiently collected at a 90° angle by a high numerical aperture fiber, resulting in a highly compact and portable device. To test the platform we performed electrophoresis and detection of a 23-mer oligonucleotide plug. Our approach is quite powerful because it allows the integration of photonic functionalities, by simple post-processing, into commercial LOCs fabricated with standard techniques.

Keywords Lab-on-a-chip · Microfluidics · Optical waveguides · Capillary electrophoresis · Laser-induced fluorescence

R. Martinez Vazquez · R. Osellame (✉) · R. Ramponi · G. Cerullo
Istituto di Fotonica e Nanotecnologie - CNR,
Dipartimento di Fisica, Politecnico di Milano,
Piazza Leonardo da Vinci, 32,
20133 Milan, Italy
e-mail: roberto.osellame@polimi.it

M. Cretich · M. Chiari
Istituto di Chimica del Riconoscimento Molecolare - CNR,
Via Mario Bianco, 9,
20131 Milan, Italy

C. Dongre · H. J. W. M. Hoekstra · M. Pollnau
Integrated Optical MicroSystems, MESA+ Institute
for Nanotechnology, University of Twente,
P.O. Box 217, 7500 AE, Enschede, The Netherlands

H. van den Vlekkert
LioniX BV,
7500 AH, Enschede, The Netherlands

Introduction

Lab-on-chips (LOCs) are microdevices aimed at the miniaturization onto a single substrate of several functionalities that typically require an entire biochemical laboratory [1–3]. In a LOC a network of microfluidic channels is used to handle very small volumes (micro- to nanolitres) of biological samples, which can be transported, mixed, separated and analysed. The LOC approach offers significant advantages over standard benchtop systems in terms of high sensitivity, speed of analysis, low sample and reagent consumption, and measurement automation and standardization. Applications of LOCs range from basic science (genomics and proteomics) to chemical synthesis and drug development [4], high-throughput medical and biochemical analysis [5], environmental monitoring and detection of chemical and biological threats.

One of the most powerful methods for the analysis of biomolecules is capillary electrophoresis (CE), in which charged molecules are separated in a microchannel as a result of their different mobilities under an applied electric field. This technique is normally performed in a glass capillary filled with buffer; CE is however particularly suited for on-chip integration [6, 7], since electrokinetic flow can be used to move and mix liquids, thus avoiding the need to integrate pumps and valves. Microchip CE (MCE) is particularly promising for clinical applications, since it allows one to perform genetic tests to diagnose a variety of diseases, both exogenous (such as bacterial or viral infections) and endogenous (detection of mutated DNA sequences related to cancer or genetically inherited diseases).

LOCs are mainly fabricated on polymer, glass or silicon substrates. Polymers are quickly becoming the most

common choice owing to their low cost and the simplicity of microchannel fabrication by molding or embossing. Nevertheless, glass is still preferred in several applications [8] as it is chemically inert, stable in time, hydrophilic, nonporous and optically clear. In particular, the choice of fused silica as the basic material adds to the previous advantages a very high optical transparency down to the UV range and a very low intrinsic fluorescence. In addition, well-established microfabrication processes, based on photolithography and etching, are available for glass.

The reduced analysis volumes in LOC systems lead to low signal levels, since fewer molecules are present in the detection region. Different detection strategies are possible, but among them the most popular is laser-induced fluorescence (LIF) which, being a background-free technique, allows the measurement of very low analyte concentrations [9]. In traditional setups used in conjunction with LOCs, both excitation and detection are performed using bulk optical equipment, such as mirrors, lenses and microscope objectives, to focus the excitation light into a tiny measurement volume and to collect the resulting fluorescence. Such schemes can provide high sensitivity, down to the single-molecule level [10, 11]; however, they require accurate mechanical alignment of the optics to the microfluidic channels, are sensitive to mechanical vibrations and drifts and allow only a limited number of detection configurations. The need to use a miniaturized LOC system in combination with a massive benchtop instrument, such as an optical microscope, undermines many of the advantages of LOCs, in particular strongly limiting device portability and preventing infield or point-of-care applications. Much of the commercial success of the LOC concept will critically depend on the ability to successfully integrate optical detection schemes. Such integration promises a significant reduction in size, cost and complexity of the system.

Several efforts have been made to integrate micro-optical components so as to perform on-chip optical detection [12, 13]. In particular, optical waveguides allow one to confine and transport light in the chip, directing it to a small volume of the microfluidic channel and to collect the emitted/transmitted light. However, the integration of optical waveguides or other photonic components with microfluidic channels is not a straightforward process, since it requires a local modification of the refractive index of the substrate. Depending on the substrate of choice, different processes are possible [14–24]. Several approaches are reported in the literature and include waveguide fabrication by silica on silicon [15–17], ion exchange in soda-lime glasses [18, 19], photolithography in polymers [14, 20] and liquid-core waveguides [21–24].

In the silica-on-silicon technology, waveguides are first fabricated on the substrate by plasma-enhanced chemical vapour deposition of core and cladding layers, followed by reactive-ion etching through a suitable mask. A further photolithographic step is then performed to etch the microchannels, which are then hermetically sealed with a cover glass. These devices were tested both for absorption [15, 17] and fluorescence [16] detection. Waveguides are multimode and have propagation losses of 1 dB cm^{-1} at 530 nm. Detection of a β-blocking agent (propranolol) by UV absorption measurements was demonstrated, with a limit of detection (LOD) of 13 μM [15]. On the other hand, exploiting fluorescence, fluorescein was detected with a LOD of 250 pM [16].

In the case of LOC in soda-lime glass, first the waveguides are fabricated by the ion-exchange technique, and then the microchannels are produced, on the same substrate, by photolithography and wet etching [18, 19]. The waveguides excite fluorescence in the fluid that fills the channels. Using a Rhodamine 6G (R6G) solution a minimum LOD of 0.5 nM was obtained, and different protein mixtures were separated and detected by LIF [18].

Several research groups used polymeric materials to combine microfluidic channels and optical waveguides. Mogensen et al. [20] fabricated the microfluidic channels and the waveguides in a single step by standard photolithography on a negative photoresist (SU-8) film, sandwiched between polymer or glass slabs. The waveguides are multimode and have propagation losses of 1.4 dB cm^{-1} at 633 nm. The device was designed to perform absorption measurements and was tested at 633 nm on channels filled with a Bromothymol Blue dye solution. This setup provided a LOD of 15 μM.

A recent approach is the use of liquid-core waveguides. Bliss et al. [21, 22] fabricated their devices by soft lithography on poly(dimethylsiloxane) (PDMS), and waveguides were created in dedicated channels by the addition of a liquid PDMS prepolymer of higher refractive index. Waveguide propagation losses are 1.8 dB cm^{-1} at 532 nm and 1.0 dB cm^{-1} at 633 nm. The device, designed for LIF applications and tested in the separation of a BK virus polymerase chain reaction product, provided a signal-to-noise ratio comparable with commercially available confocal-based systems.

Yin et al. [23, 24] fabricated a device based on planar networks of intersecting solid- and liquid-core waveguides, where the fluorescent molecules are inside the “liquid” core, and both types of waveguides are used to deliver and collect the excitation and fluorescence light. Fluorescently labelled liposomes are used to demonstrate single-molecule detection by fluorescence correlation spectroscopy.

From the previous examples it can be concluded that the fabrication of optical waveguides integrated with the microfluidic channels is not a straightforward process. Since the production of optical waveguides requires a localized increase of the refractive index in the device

volume, whatever technology is chosen, it strongly affects the fabrication procedure of the microfluidic part of the chip. In addition, the complex patterning of the surface, required by the simultaneous fabrication of the microchannels and the optical waveguides, introduces challenging technical problems in sealing the devices.

A novel technique has recently emerged for the direct writing of waveguides and photonic circuits in transparent glass substrates by focused femtosecond pulses [25–31]. The ultrashort pulse duration ($\approx 10^{-13}$ s) leads to very high peak powers (≈10 MW) and intensities ($\approx 10^{14}$ W cm^{-2}), when focused by a microscope objective, even for low average powers (tens of mW). Due to such high intensities, the interaction of the laser pulse with the material becomes strongly nonlinear; in particular a very selective absorption (due to a combination of multiphoton and avalanche ionization processes) occurs only in a small volume around the focus, where the intensity is the highest, allowing highly spatially selective energy deposition. The hot electron plasma induces high temperatures and pressures that give rise to structural modifications such as densification and creation of colour centres [27]. The combination of all these effects leads, under suitable conditions, to a local increase of the refractive index, which can be exploited, by moving the laser focus inside the substrate, in order to produce three-dimensional light-guiding structures.

Compared with traditional techniques, femtosecond waveguide writing in a glass chip offers two striking advantages: (i) it is a direct maskless fabrication technique, i.e. in a single step one can create optical waveguides or more complicated photonic devices (splitters, interferometers, etc.) by moving the sample with respect to the laser focus; (ii) it is a three-dimensional technique, since it allows one to define waveguides at arbitrary depths inside the glass. So far, this technique has been almost exclusively applied to the manufacturing of optical waveguides for telecom photonic devices [28, 29]. However, it appears highly suited for the integration of optical waveguides into LOCs. In fact, it is possible to locate optical waveguides at arbitrary positions inside a microfluidic device, thus allowing waveguide–channel and waveguide–waveguide crossing on different planes if intersection is to be avoided; in this way more compact layouts are feasible and much more freedom in the design is possible. In addition, it can be applied to a prefabricated LOC without affecting the layout and the manufacturing procedure of the microfluidic part of the device, thus greatly simplifying the production process and taking advantage of the several existing, well-developed designs for microfluidic chips. Finally, the flexibility of this technology brings evident advantages in terms of rapid prototyping and customization of the optofluidic devices; in fact, once the microfluidic performance is assessed, the position and the number of the waveguides providing the excitation/collection of light can be experimentally optimized in a very easy way or varied on demand according to the customer needs.

In this paper we demonstrate the integration of femtosecond-laser-written optical waveguides into a commercial glass LOC. We fabricate high-quality waveguides intersecting the microfluidic channels at arbitrary positions and use them to optically address their content with high spatial selectivity. In particular, we apply our technique to integrate optical detection in a microchip designed for MCE: waveguides are inscribed at the end of the separation channel in order to optically excite the different plugs reaching that point; fluorescence from the labelled biomolecules crossing the waveguide output is efficiently collected at a 90° angle by a high numerical aperture optical fiber. The device performance is validated by detecting plugs of dye-labelled oligonucleotides at different concentrations. With respect to previous works we demonstrate the feasibility of the femtosecond laser writing for waveguide fabrication in LOCs; this technology not only brings all the advantages previously discussed but in the meantime provides state of the art results in terms of detection sensitivity. Present results pave the way to highly compact and portable LOC devices with applications to clinical or point-of-care diagnostics.

Materials and methods

Chemicals

Rhodamine 6G was bought from Exciton (USA). Oligonucleotides were purchased from MWG (Germany). Epoxy-polydimethylacrylamide (EPDMA) was synthesized as described elsewhere [32].

Microfluidic chips

We used a commercial fused silica microfluidic chip for CE (model D8-LIF from LioniX BV) that is 64.0×5.5 mm^2 in size and 1.0-mm thick. The microchannels are manufactured by photolithography followed by wet etching and then sealed by a cover glass slab. The microchannels are located 500 μm below the chip surface and have a nearly rectangular cross section with 50-μm width and 12-μm height.

The layout of the chip is shown in Fig. 1a: it consists of two crossing microchannels that are responsible for sample injection (channel going from reservoir 1 to 3) and separation (channel going from reservoir 2 to 4). The microchannels are folded in a complex way to reduce the chip footprint. The distance between the crossing point and reservoir 4, i.e. the maximum separation distance, is 68.6 mm.

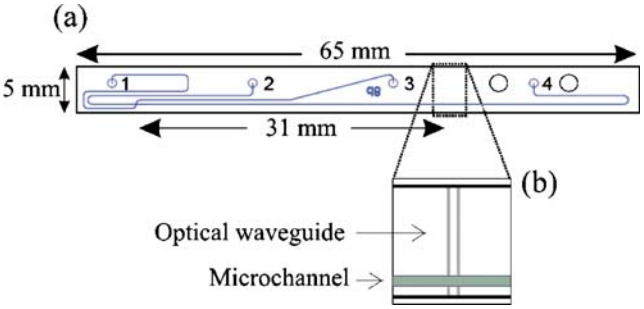

Fig. 1 *a* Layout of the CE microfluidic chip with the most significant dimensions; *1–4* label the four reservoirs at the end of the two crossing channels. *b* Blowup of the region where the femtosecond-laser-written waveguide crosses the separation channel

To perform CE measurements the chip is inserted in a commercial cartridge providing reservoir connections and electrical contacts (MCC-1 of the Capella platform, CapiliX BV) and in turn connected to the Capella Programmable Power Supply Unit-4 (PSU-4) that applies the voltages (from 0 to 2 kV) to the different reservoirs of the CE chip. The PSU-4 unit allows one to control the entire on-chip flow with a Labview script and applying voltages with a switching time of 10 ms; in addition, the same unit provides measurements of the currents inside the microchannels with a resolution of 0.1 μA.

Femtosecond laser writing

Figure 2 is a schematic of the experimental setup used for the fabrication of the waveguides. It starts with a regeneratively amplified Ti:sapphire laser that produces 150-fs, 500-μJ pulses at 1 kHz and 800 nm. A fraction of the pulse energy, ranging from 2 to 5 μJ and adjusted with a variable attenuator, is used for waveguide writing. In order to obtain waveguides with circular cross section, the beam is astigmatically shaped by passing it through a cylindrical telescope, according to a previously reported method [33]. The beam is then focused by a ×20 microscope objective (numerical aperture NA=0.3) at a depth variable from 0.2 to 1 mm inside the microfluidic chip. The sample is moved perpendicularly to the beam propagation direction by a precision translation stage at a speed varying from 10 to 100 μm s^{-1}.

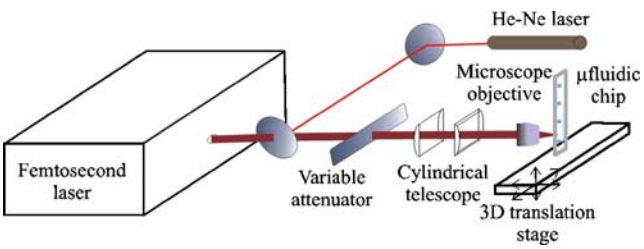

Fig. 2 Experimental setup for optical waveguide writing. The superimposed He–Ne laser is used for alignment of the sample, and the cylindrical telescope provides the astigmatic beam shaping necessary for circular cross section waveguides

Coating procedure

The protocol used for coating the inner walls of the microfluidic channels is based on the dynamic adsorption of EPDMA [32]. Briefly, a pretreatment of the chip with a 0.1 M solution of NaOH for 30 min was followed by a 30-min treatment with a 0.6 % w/v solution of EPDMA in 12% w/v ammonium sulphate. The EPDMA solution was introduced into the channel by applying vacuum to one reservoir while keeping the other three reservoirs filled with the EPDMA solution.

Laser-induced fluorescence detection setup

Our excitation/detection system is shown in Fig. 3: it combines compactness, portability, high sensitivity and strong background rejection. An optical waveguide is inscribed perpendicular to the separation channel towards

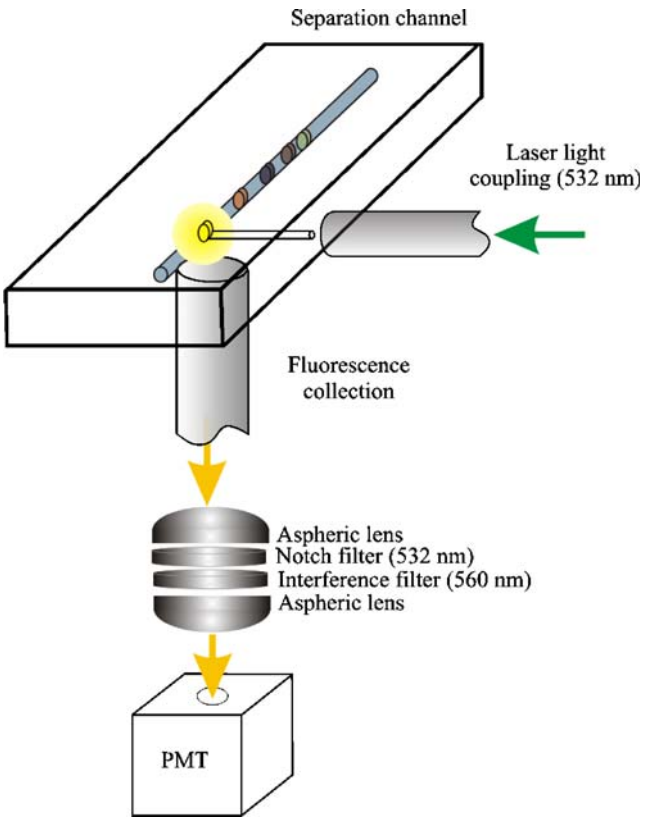

Fig. 3 Scheme of the setup used for the LIF experiments, with two optical fibers for fluorescence excitation and collection. The collected fluorescence is then detected by a photomultiplier tube (*PMT*) after suitable filtering

its end, in order to selectively excite a small volume of the fluid, thus providing a photofinish for the separated plugs. Light from a CW green laser (model 4301-010, Uniphase) is coupled into the waveguide by an optical fiber.

The fluorescence from the excited volume is collected by a second optical fiber placed perpendicularly to the excitation waveguide, in order to minimize the background from the excitation light. We used an optical fiber, rather than a second inscribed waveguide, to collect the fluorescence, because: (a) the path to the microchip surface is only 500 μm; (b) femtosecond-laser-written waveguides have relatively low numerical aperture (NA≈0.1) and thus are not suitable for efficient light collection. Both the NA and the diameter of the detection fiber were selected in order to maximize the collected fluorescence and minimize stray light. In the following we consider the excited portion of the microchannel, from where fluorescence is emitted, as a point source. The light collection efficiency (LCE), defined as the fraction of isotropic fluorescence collected by the optical system, is given by

$$\mathrm{LCE} = \Omega/4\pi = 1/2(1-\cos\theta_{\max}), \tag{1}$$

where Ω is the solid angle subtended by the collection optics, corresponding to a half cone with angle $\theta_{\max}$. This angle can be related to the numerical aperture of the optical fiber by

$$\mathrm{NA} = n_0 \sin\theta_{\max}, \tag{2}$$

where n_0 is the refractive index of the medium from which the signal is collected (considered as glass in our case with $n_0 \approx 1.45$). One can then write:

$$\mathrm{LCE} = \frac{1}{2}\left[1-\sqrt{1-\left(\frac{\mathrm{NA}}{n_0}\right)^2}\right] \tag{3}$$

For NA=0.5 we achieve an LCE of 3%, which is comparable with that achieved with a standard microscope objective, with the advantage of added integration and system portability.

An additional constraint to be satisfied is that the fiber cross section should be large enough to intercept all the rays contained within $\theta_{\max}$. Assuming the fluorescence as a point source located at a distance d below the chip surface, and calling a the fiber radius, one obtains

$$a \geq d\ \tan\theta_{\max} = \frac{d\frac{\mathrm{NA}}{n_0}}{\sqrt{1-\left(\frac{\mathrm{NA}}{n_0}\right)^2}} \tag{4}$$

For the numerical values relevant to our case (d= 500 μm) we obtain $a \geq 180$ μm. We used a collection fiber with NA=0.48 and a core radius of 300 μm (model HWF-H-600T, Ceram Optec), which satisfies both requirements. It has a fused silica core, to minimize background fluorescence, and a polymer cladding to provide high refractive index contrast.

The light from the fiber is collimated by an aspherical lens (focal length f=20 mm, NA=0.54), filtered by a notch filter (Semrock, model NF01-532U-25) and an interference filter (Corion, model 560-101-6952, 10-nm bandwidth at 560 nm), and finally refocused by a second aspherical lens (same characteristics as the first one) into a photon-counting photomultiplier (PMT, Hamamatsu, model H7421-40, dark counts ≈ 40 cps) and read out by a data acquisition board (National instruments, model PCI6013). Dynamic fluorescence measurements are typically performed with an integration time of 30 ms.

Results and discussion

Waveguide fabrication

We first optimised the waveguide fabrication parameters using plain fused silica substrates of the same quality as those used for LOC production. The optimum waveguides were obtained with a pulse energy of 4 μJ and a translation speed of 20 μm s^{-1}. They displayed a refractive index increase of $\approx 10^{-3}$, corresponding to single-mode operation throughout the visible region with mode diameter of 11 μm, well matched to the microfluidic channel height of 12 μm. The propagation losses, measured with the cutback technique, were found to be 0.9 dB cm^{-1} at 532 nm [34]. This value is very promising compared with those obtained at similar wavelengths in waveguides integrated in LOCs [14–24], and is fully adequate for the biosensing application.

When performing MCE experiments, the separated microfluidic plugs are typically detected at the end of the separation channel by LIF. Therefore we set out to fabricate, by using the femtosecond laser, a series of waveguides perpendicular to the separation channel towards its end (see Fig. 1b), i.e. at 31 mm from the crossing point. This post-processing ability is a unique feature of the femtosecond waveguide writing approach and represents one of its main strengths.

The depth positioning of the waveguides with respect to the microchannel is quite critical, so a specific alignment procedure was developed. A reference position is taken on the back surface of the sample at the focus position where ablation is obtained. Since ablation relies on a non-linear absorption process, the precision in determining the reference position is much higher than the confocal parameter of the focussing objective. From this position the focus of the writing beam is moved inside the sample by a precalibrated distance in order to reach the microchannel; this procedure results in a positioning accuracy

higher than 2 μm in the depth direction, thus allowing a nearly perfect waveguide–channel alignment.

Limit of detection of the LIF setup

The sensitivity of the integrated optical detection system was first evaluated by filling the chip with a solution of Rhodamine 6G (R6G) dissolved in a phosphate buffer (pH 7.2). Figure 4 shows a microscope image of the yellow fluorescence for a R6G concentration of 10 μM. The image demonstrates the high spatial selectivity of the excitation (11 μm, as the waveguide mode), and the very low leakage out of the waveguide, which is quite important for a high spatial resolution in the CE experiments. In addition, the excited fluorescence covers the whole width (50 μm) of the channel owing to the low divergence of the excitation light coming from the waveguide. It is worth noting that the low NA of the femtosecond-laser-written waveguides, which may represent a limitation for fluorescence collection, is indeed a great advantage when excitation through relatively large channels is required. These results demonstrate the capability of the integrated optical waveguide to achieve highly spatially selective excitation of the contents of the microfluidic channel.

In order to obtain the static LOD of our system, the chip was filled with progressively higher concentrations of R6G. Fluorescence was excited with a fixed laser power coupled into the waveguide (100 μW). We obtained a minimum detectable fluorophore concentration of 40 pM, which is among the best values reported in the literature for integrated optical detection setups [14]. The sensitivity is currently limited by the background signal, measured in a channel filled with buffer. This background is attributed to:

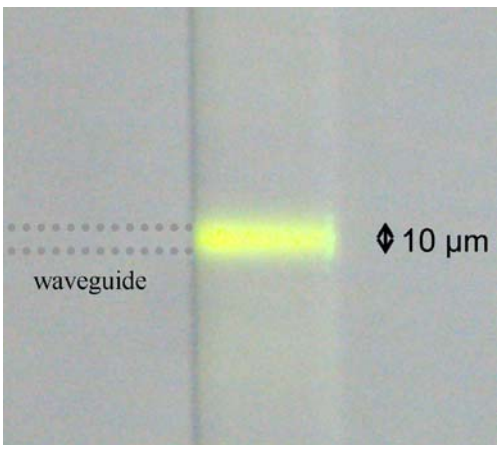

Fig. 4 Microscope image of fluorescence from a microfluidic channel in a commercial LOC, excited by an optical waveguide orthogonal to the channel. The microchannel is filled with R6G, while the waveguide is not visible due to the low refractive index contrast. A long-pass filter rejects the 532-nm excitation light

(a) autofluorescence and Raman scattering from the fused silica substrate; (b) scattering from the unpolished side surfaces of the chip. Work is in progress to reduce this background by optimizing the fused silica quality and polishing the chip side walls; it is however worth noting that the current LOD corresponds to only 150 dye molecules in the excitation volume, demonstrating the high quality of the integrated detection setup.

Electroosmotic flow suppression

In most MCE applications it is necessary to control the electroosmotic flow (EOF) to achieve optimal separation. For example, at high pH, the EOF may be too rapid, resulting in the elution of the sample before separation has occurred. Conversely, at low pH the EOF may be too slow allowing interactions between the negatively charged and cationic solutes. EOF depends strongly on the quality of the walls of the microchannels. As a consequence, small defects in the walls will create “turbulences” in the EOF that will affect the MCE experiment by broadening the injected plugs [35]. An effective modification of surface properties can be achieved by coating the walls of the microchannels with a polymer. Neutral polymers, chemi- or physisorbed on the wall, strongly decrease EOF by shielding surface charge and by increasing local viscosity. To coat the microchannels of our MCE chip we have used a method based on the dynamic adsorption of EPDMA, already used with success in other microfluidic chips [36].

The current monitoring method [37] was used to measure EOF in the microchip channels, before and after coating. We used a phosphate/Na^+ buffer solution, with pH 7.21, at two different concentrations, 50 and 25 mM. First the microchannels were filled with the higher-conductivity buffer (50 mM) applying vacuum at reservoir 4 until no air bubbles were observed. Then a voltage of 1,200 V was applied to reservoirs 1, 2 and 3 for 5 min to determine the baseline current. Afterwards reservoir 2 was emptied and filled with the 25 mM buffer, a voltage of 1,000 V was applied for 1,500 s, and the current was measured. If EOF is present, the lower-conductivity buffer replaces the initial higher-conductivity one and a current drop is observed. By measuring the time τ required to replace the higher-conductivity buffer with the lower-conductivity one, the electroosmotic mobility (μ_{eo}) is obtained as

$$\mu_{eo} = L^2/(V\tau), \tag{5}$$

where V is the applied voltage, and L is the microchannel length, in our case 9.4 cm.

As an example, Fig. 5a reports the current measured in an uncoated microchip as a function of time, and Fig. 5b reports that of a coated one. From the measurement

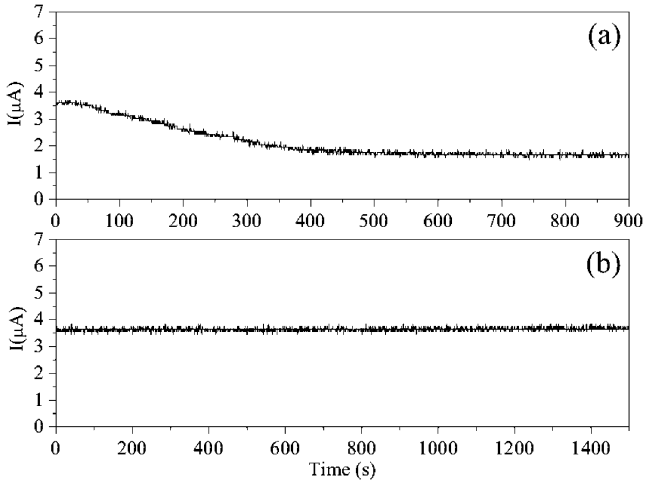

Fig. 5 Current-monitoring experiments for EOF characterization. Current measured in **a** an uncoated and **b** coated microchip as a function of time

in the uncoated microchip we estimated a μ_{eo} of 2.5×10^{-8} m^2 V^{-1} s^{-1}. Figure 5b shows that there is no drop in the current after 1,500 s, demonstrating an effective EOF suppression on the timescale of our experiments.

MCE of an oligonucleotide with integrated optical detection

The MCE setup with integrated optical detection described in this paper was finally tested by performing injection and electrophoresis of a 23-mer Cy3-labelled oligonucleotide plug.

Figure 6 shows two electropherograms corresponding to different oligonucleotide concentrations (10 nM and 1 nM). The effective laser excitation power incident on the waveguide was 100 μW in both cases.

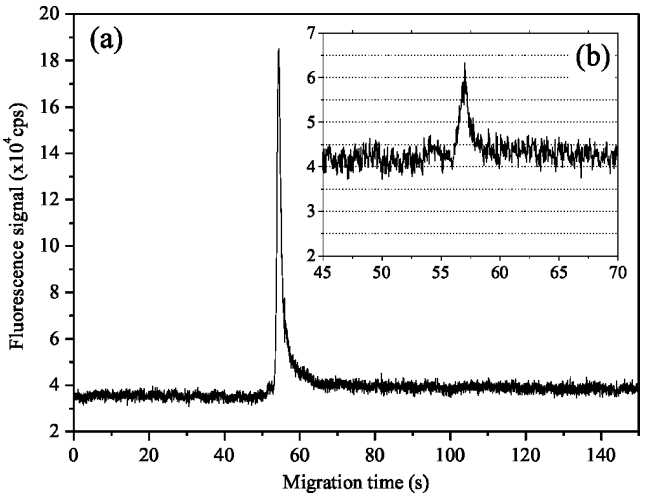

Fig. 6 Electrophoresis of a 23-mer Cy3-labelled oligonucleotide at a concentration of *a* 10 nM and *b* 1 nM, in a microchip coated with EPDMA

A quantitative estimation of the sensitivity of the device can be obtained from the signal-to-noise ratio (S/N) of the measurement [38], defined as

$$\mathrm{S/N} = \left(C_\mathrm{p} - C_\mathrm{B}\right)/\sigma_\mathrm{B}, \tag{6}$$

where C_p is the peak counting rate, C_B the average background count rate, and σ_B the standard deviation of the background signal. In Fig. 6b we have $\sigma_\mathrm{B}\approx$2,000 cps, so that the S/N is 10. Since the shot noise of the background is $(C_\mathrm{B})^{1/2} \approx 200$, the sensitivity of our device is not limited by shot noise but by other noise sources such as laser power fluctuations. This means that using a more stable laser we should be able to decrease the sensitivity by at least 10 times, reaching a minimum detectable oligonucleotide concentration of ≈100 pM.

The width of the peak in the electropherogram allows us to estimate the length of the plug at the detection point. As the distance from the waveguide to the crossing point is 31 mm, and assuming a constant velocity, we obtain a plug length of 1 mm when it passes in front of the waveguide. When the plug enters the separation channel it has about the same length as the microchannel width, i.e. 50 μm, thus it undergoes a significant broadening during migration. This broadening is quite standard in MCE experiments and can be mainly attributed to diffusion. Additional causes of dispersion of the plug are Joule heating generated by the passage of electrical currents along the buffer and residual sample adsorption at the channel walls, which also explains the peak asymmetry [35].

The stability of the coating was assessed by repeated injections and separation of the oligonucleotide. It allowed 30 measurements before the EOF appeared again. Rinsing the channel with a highly concentrated NaOH solution (1 M) totally removed the spoiled coating. Subsequently, a second coating of the microchannel was possible and allowed us to reuse the same chip for 30 additional runs.

Conclusions

We have used femtosecond laser writing to fabricate high-quality optical waveguides in a fused silica MCE chip and demonstrated their capability to excite fluorescent molecules flowing in the microfluidic channels with high spatial selectivity. Our approach is quite powerful because it allows the integration of photonic functionalities by simple post-processing of commercial LOCs, fabricated with standard techniques. This method has allowed us to develop a highly integrated detection scheme that allows the observation of low-concentration fluorescent solutions. The coating of the microchannel walls permits one to perform electrophoresis of a Cy3-labelled oligonucleotide

with limited plug broadening. The innovative fabrication technology based on femtosecond laser writing of waveguides and the fluorescence excitation/detection scheme demonstrated here could strongly increase the portability and compactness of the LOCs by overcoming the present limitation where microfluidic systems are coupled to macroscopic bulk optical detection systems.

Acknowledgements This work was funded by the European Commission, 6th FP STREP Project Contract No. IST-2005-034562 [Hybrid Integrated Biophotonic Sensors Created by Ultrafast laser Systems (HIBISCUS)].

References

1. Reyes RD, Iossifidis D, Auroux PA, Manz A (2002) Anal Chem 74:2623–2636
2. Auroux PA, Reyes DR, Iossifidis D, Manz A (2002) Anal Chem 74:2637–2652
3. Whitesides GM (2006) Nature 442:368–373
4. de Mello AJ (2006) Nature 442:394–402
5. Yager P, Edwards T, Fu E, Helton K, Nelson K, Tam MR, Weigl BH (2006) Nature 442:412–418
6. Harrison DJ, Fluri K, Seiler K, Fan ZH, Effenhauser CS, Manz A (1993) Science 261:895–897
7. Landers JP (2003) Anal Chem 75:2919–2927
8. Dishinger JF, Kennedy RT (2007) Anal Chem 79:947–954
9. Mogensen KB, Klank H, Kutter JP (2004) Electrophoresis 25:3498–3512
10. Craighead H (2006) Nature 442:387–393
11. de Mello AJ (2003) Lab Chip 3:29N–34N
12. Verpoorte E (2003) Lab Chip 3:42N–52N
13. Hunt HC, Wilkinson JS (2008) Microfluid Nanofluid 4:53–79
14. Kuswandi B, Nuriman, Huskens J, Verboom W (2007) Anal Chim Acta 601:141–155
15. Mogensen KB, Friis P, Hübner J, Petersen NJ, Jorgensen AM, Telleman P, Kutter JP (2001) Opt Lett 26:716–718
16. Hubner J, Mogensen KB, Jorgensen AM, Friis P, Telleman P, Kutter JP (2001) Rev Sci Instrum 72:229–234
17. Mogensen KB, Petersen NJ, Hübner J, Kutter JP (2001) Electrophoresis 22:3930–3938
18. Mazurczyk R, Vieillard J, Bouchard A, Hannes B, Krawczyka S (2006) Sens Act B 118:11–19
19. Vieillard J, Mazurczyk R, Morin C, Hannes B, Chevolot Y, Desbene PL, Krawczyk S (2007) J Chromatogr B 845:218–225
20. Mogensen KB, El-Ali J, Wolff A, Kutter JP (2003) Appl Opt 42:4072–4079
21. Bliss CL, McMullin JN, Backhouse CJ (2007) Lab Chip 7:1280–1287
22. Bliss CL, McMullin JN, Backhouse CJ (2008) Lab Chip 8:143–151
23. Yin D, Deamer DW, Schmidt H, Barber JP, Hawkins AR (2006) Opt Lett 31:2136–2138
24. Yin D, Lunt EJ, Rudenko MI, Deamer DW, Hawkins AR, Schmidt H (2007) Lab Chip 7:1171–1175
25. Davis KM, Miura K, Sugimoto N, Hirao K (1996) Opt Lett 21:1729–1731
26. Itoh K, Watanabe W, Nolte S, Schaffer C (2006) MRS Bull 31:620–625
27. Gatass RR, Mazur E (2008) Nature Photon 2:219–225
28. Osellame R, Chiodo N, Della Valle G, Cerullo G, Ramponi R, Laporta P, Killi A, Morgner U, Svelto O (2006) J Select Topics Quantum Electron 12:277–285
29. Eaton SM, Chen W, Zhang L, Zhang H, Iyer R, Aitchison JS, Herman PR (2006) IEEE Photon Technol Lett 18:2174–2176
30. Cai B, Komatsu K, Sugihara O, Kagami M, Tsuchimori M, Matsui T, Kaino T (2008) Appl Phys Lett 92:253302
31. Wang Z, Sugioka K, Hanada Y, Midorikawa K (2007) Appl Phys A 88:699–704
32. Chiari M, Cretich M, Damin F, Cerotti L, Consonni R (2000) Electrophoresis 21:909–916
33. Osellame R, Taccheo S, Marangoni M, Ramponi R, Laporta P, Polli D, De Silvestri S, Cerullo G (2003) J Opt Soc Am B 20:1559–1567
34. Osellame R, Maselli V, Martinez Vazquez R, Ramponi R, Cerullo G (2007) Appl Phys Lett 90:231118
35. Ghosal S (2004) Electrophoresis 25:214–228
36. Cretich M, Chiari M, Rech I, Cova S (2003) Electrophoresis 24:3793–3799
37. Huang X, Gordon MJ, Zare RN (1988) Anal Chem 60:1837–1838
38. Rech I, Cova S, Restelli A, Ghioni M, Chiari M, Cretich M (2006) Electrophoresis 27:3797–3804